Anomalous celestial polarization caused by forest fire smoke: why do some insects become visually disoriented under smoky skies?

Ramón Hegedüs, Susanne Åkesson, and Gábor Horváth

The effects of forest fire smoke on sky polarization and animal orientation are practically unknown. Using full-sky imaging polarimetry, we therefore measured the celestial polarization pattern under a smoky sky in Fairbanks, Alaska, during the forest fire season in August 2005. It is quantitatively documented here that the celestial polarization, a sky attribute that is necessary for orientation of many polarization-sensitive animal species, above Fairbanks on 17 August 2005 was in several aspects anomalous due to the forest fire smoke: (i) The pattern of the degree of linear polarization p of the reddish smoky sky differed considerably from that of the corresponding clear blue sky. (ii) Due to the smoke, p of skylight was drastically reduced ($p_{max} \leq 14\%$, $p_{average} \leq 8\%$). (iii) Depending on wavelength and time, the Arago, Babinet, and Brewster neutral points of sky polarization had anomalous positions. We suggest that the disorientation of certain insects observed by Canadian researchers under smoky skies during the forest fire season in August 2003 in British Columbia was the consequence of the anomalous sky polarization caused by the forest fire smoke.

OCIS codes: 010.1290, 110.2960, 120.5410, 280.1310, 330.7310.

1. Introduction

Forest fires and their environmental effects constitute important subjects of current research.[1–4] The disadvantageous effects of smoke and other combustion products of huge and long-lasting forest fires in triggering weather fluctuations and contributing to global climate change cannot be excluded.[1,3–5] Apart from causing huge damage to the local economy and biodiversity, as well as health problems to humans, large-scale forest fires also release a huge amount of carbon into the atmosphere, contributing considerably to the annual increase in atmospheric carbon dioxide.[6–8] The most immediate consequence of forest fires is the diminution of direct solar radiation due to the absorption by smoke, which decreases the solar energy available for plant photosynthesis and solar power plants.[9] The most spectacular consequences of forest fires are some striking color phenomena in the sky visible with the naked eye, like the red sky during the day (Fig. 1), colorful rings around the Sun, or beautifully colored sunset glows.[10] These atmospheric optical phenomena induced by forest fire smoke are very similar to those caused by dust clouds produced by volcanic eruptions.[10–12]

Although the effects of volcanic dust clouds on the environment are relatively well studied and documented,[10,13–15] the effects of forest fire smoke on atmospheric optical phenomena and animal orientation are almost unknown. However, it is likely that a deviating polarization pattern caused by forest fire smoke will have negative effects on navigation performance and motivation to migrate in invertebrate and vertebrate fauna dependent on skylight polarization for compass information.[16–18] Recently, Johnson *et al.*[19] reported on the environmental effects of Canadian forest fires in August 2003, when in British Columbia over 1.5 million hectares of forest burned in over 2000 separate fires. Aerosols, consisting of suspended ash particles, concentrated in valleys and moved east onto the prairies. Smoke darkened the sky, and many insects reduced straight-line flying to short distances only. Flights by grasshoppers (Orthoptera: Acrididae) were greatly reduced. A previously uncommon, but locally occurring seed bug

R. Hegedüs and G. Horváth (gh@arago.elte.hu) are with the Biooptics Laboratory, Department of Biological Physics, Physical Institute, Loránd Eötvös University, H-1117 Budapest, Pázmány Péter sétány 1, Hungary. S. Åkesson is with the Department of Animal Ecology, Lund University, Ecology Building, SE-223 62 Lund, Sweden.

Received 19 October 2006; revised 6 December 2006; accepted 18 December 2006; posted 3 January 2007 (Doc. ID 76241); published 23 April 2007.

0003-6935/07/142717-10$15.00/0

Fig. 1. (Color online) Photograph of the reddish, smoky sky taken at the airport of Fairbanks on 17 August 2005 at 10:20 h (local summer time = UTC − 8).

(*Sphragisticus nebulosus*: Hemiptera: Rhyparochromidae) fledged, but delayed flight, building up in large numbers in the southern Alberta grassland. When skies cleared, mass bug migrations invaded the city of Medicine Hat, Alberta, in sufficient numbers to close stores and restaurants.

To understand the polarization characteristics of the smoky sky, we measured the celestial polarization pattern by full-sky imaging polarimetry in Fairbanks, Alaska, during several separate forest fires in the vicinity (Fig. 2). We document here quantitatively how the celestial polarization, a sky attribute that is necessary for orientation of many polarization-sensitive animal species,[17] changed due to the forest fire smoke. In Section 4, we suggest that the disorientation of insects observed by Johnson *et al.*[19] under smoky skies was the consequence of the anomalous sky polarization caused by forest fire smoke.

2. Materials and Methods

The anomalous sky polarization patterns (Figs. 3 and 4, Table 1) were measured on 17 August 2005 at 15:01, 16:25, 18:02, and 20:20 h (local summer time = UTC − 8) in Fairbanks, Alaska (64° 49′ N, 147° 45′ W), at the beginning of the third part (leg 3) of the international arctic polar research expedition Beringia 2005 organized by the Swedish Polar Research Secretariat. The celestial polarization measurements could be collected only at these four points of time and could not be repeated later, because the expedition stayed only some hours in Fairbanks for transit. The polarization patterns of a clear, nonanomalous sky (Fig. 5) were measured above the arctic ice cover on 25 August 2005 at 21:20 h (= UTC − 8) at 78° 28′ N and 149° 9′ W.

The skylight polarization was measured by full-sky imaging polarimetry, the technique, calibration, and evaluation procedure of which have been described in detail by Gál *et al.*[20] A 180° field of view (full sky) was ensured by a fish-eye lens (Nikon-Nikkor, $F = 2.8$, focal length of 8 mm) with a built-in rotating disk mounted with three broadband (275–750 nm) neutral-density linearly polarizing filters (Polaroid HNP'B) with three different polarization axes (0°, 45°, and 90° from the radius of the disk).

The detector was a photoemulsion (Kodak Elite Chrome ED 200 ASA color reversal film; the maxima and half-bandwidths of its spectral sensitivity curves were $\lambda_{red} = 650 \pm 40$ nm, $\lambda_{green} = 550 \pm 40$ nm, $\lambda_{blue} = 450 \pm 40$ nm) in a roll-film photographic camera (Nikon F801). For a given sky, three photographs were taken for the three different directions of the transmission axis of the polarizers. The camera was set on a tripod such that the optical axis of the fish-eye lens was vertical, i.e., pointed to the zenith. After 24-bit (3×8 for red, green, and blue) digitization (by a Canon Arcus 1200 scanner) of the three chemically developed color pictures for a given sky and their computer evaluation, the patterns of the radiance I, degree of linear polarization p, and angle of polarization α (or E-vector alignment) of skylight were determined as color-coded, two-dimensional, circular maps, in which the center is the zenith, the perimeter is the horizon, and the zenith angle θ is proportional to the radius from the zenith (horizon: $\theta = 90°$, zenith: $\theta = 0°$). These patterns were obtained in the red, green, and blue spectral ranges, in which the three color-sensitive layers of the photoemulsion used have maximal sensitivity. The degree p and angle α of linear polarization were measured by our polarimeter with an accuracy of $\Delta p = \pm 1\%$ and $\Delta\alpha = \pm 2°$, respectively.

The theoretical α patterns of the clear sky (Figs. 3B, 4B, and 5B) were calculated on the basis of the model of Berry *et al.*,[21] which provides a good quantitative approximation of experimental clear sky α patterns, particularly with respect to the existence of neutral points. The model has three parameters to be freely set: two for the Sun position (solar zenith and azimuth angles) and one for the angular distance (digression) between the Arago and the Brewster neutral points. In our case, the theoretical α patterns were computed according to the position of the Sun as it appears on the photographs (Figs. 3A and 5A) or estimated on the basis of the exact time and geographical coordinates of the site of measurements (Fig. 4A). The digression between the Arago and Brewster points was set to 40°. Thus the theoretical α patterns in Figs. 3B, 4B, and 5B show how the celestial E-vector distribution at the time of measurements were expected to appear under clear-sky conditions without the atmospheric effect of the forest fire smoke and smoke-induced fog.

The noisiness n of a given α pattern (Table 1) was calculated as follows: The α patterns were scanned throughout with a window of 5 pixels $\times$ 5 pixels, in which the standard variance (σ^2) of the angle of polarization α was calculated, and then the average of the standard variances of all 5 pixel $\times$ 5 pixel windows was obtained. Finally, this value was normalized to that of white noise calculated with the same method. Thus, noisiness n of an α pattern denotes how noisy it is compared with the white noise (n = 0%: no noise, n = 100%: white noise).

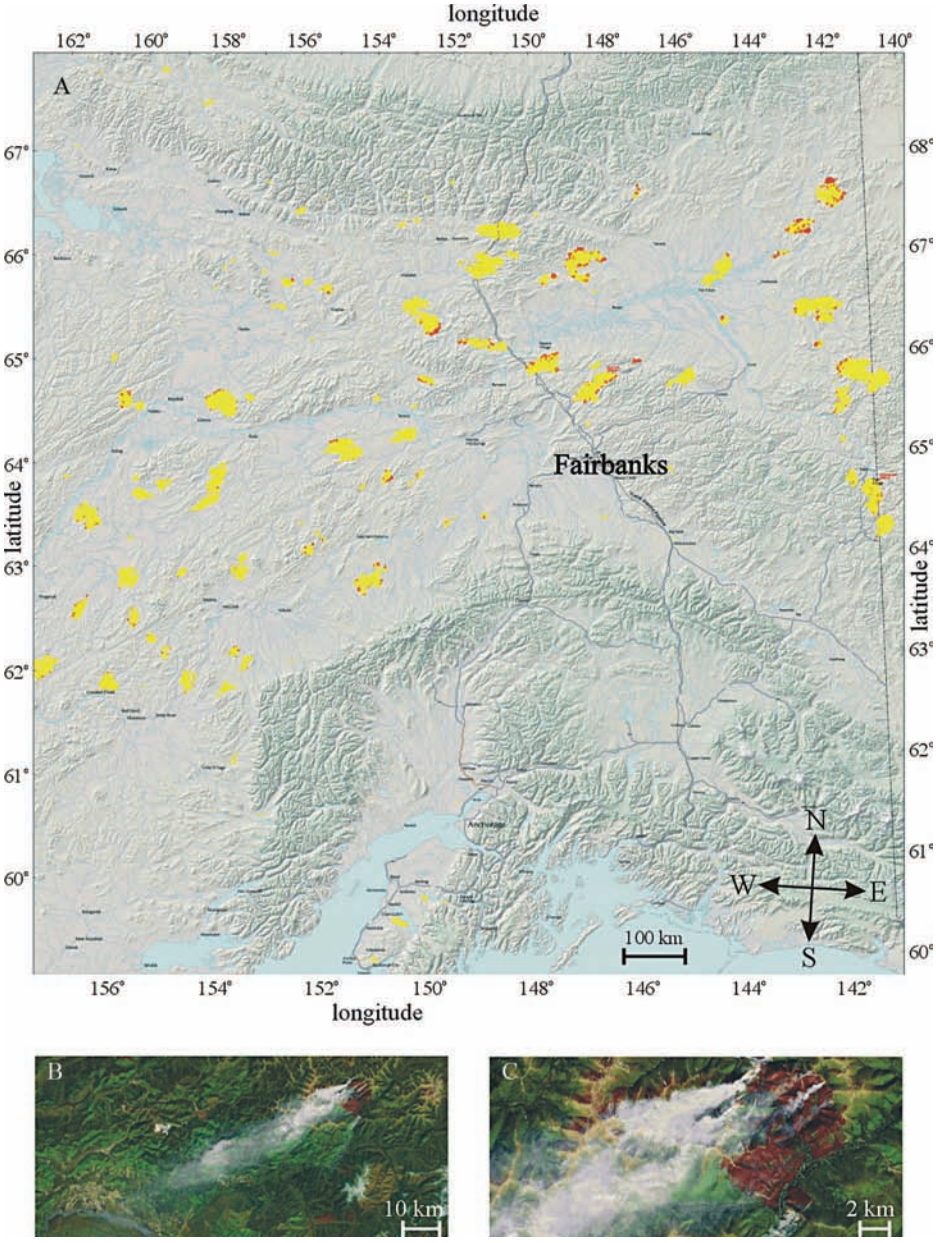

Fig. 2. (Color online) A, Locations of forest fires (red spots) in the vicinity of Fairbanks on 17 August 2005 at 15:00 h (local summer time = UTC − 8) displayed on the geographical map of interior Alaska. Data from the MODIS Active Fire Detection (http://activefiremaps.fs.fed.us). Yellow: previously (since 1 January 2005) burned areas. Orange: actively burning areas (last 24 h). Red: actively burning areas (last 12 h). B, C, Satellite photographs of a forest fire in the vicinity of Fairbanks [Google—Imagery © 2005 Digital Globe (http://maps.google.com)].

3. Results

On 17 August 2005, the sky above Fairbanks was cloudless, but smoky and foggy (Figs. 1 and 2). The Sun disk was visible from 10 to 18 h, but during the fourth (last) polarimetric measurement, at 20:20 h, the Sun was not discernible due to the thick smoke and fog and the low solar elevation. The sky color was whitish gray with a slight pink tint (Figs. 1, 3A, and 4A). The radiance I of the reddish skylight was highest in the red spectral range, lower in the blue, and lowest in the green (Table 1). Contrary to the anomalous pink sky color, the nonanomalous, clear sky above the arctic ice was blue (Fig. 5A); its radiance increased considerably with decreasing wavelength (Table 1).

The degree of linear polarization p of light from the smoky sky was also anomalous, because it was very low in all three spectral ranges (Table 1): Depending on the wavelength and time, the average of p changed between 4% and 8%, and the standard deviation of p ranged from 3% to 6%. Contrary to this, the average p of light from the clear, nonanomalous sky was between 21% and 34% (Table 1), and its maximum was higher than 67% in the red spectral range (Fig. 5C).

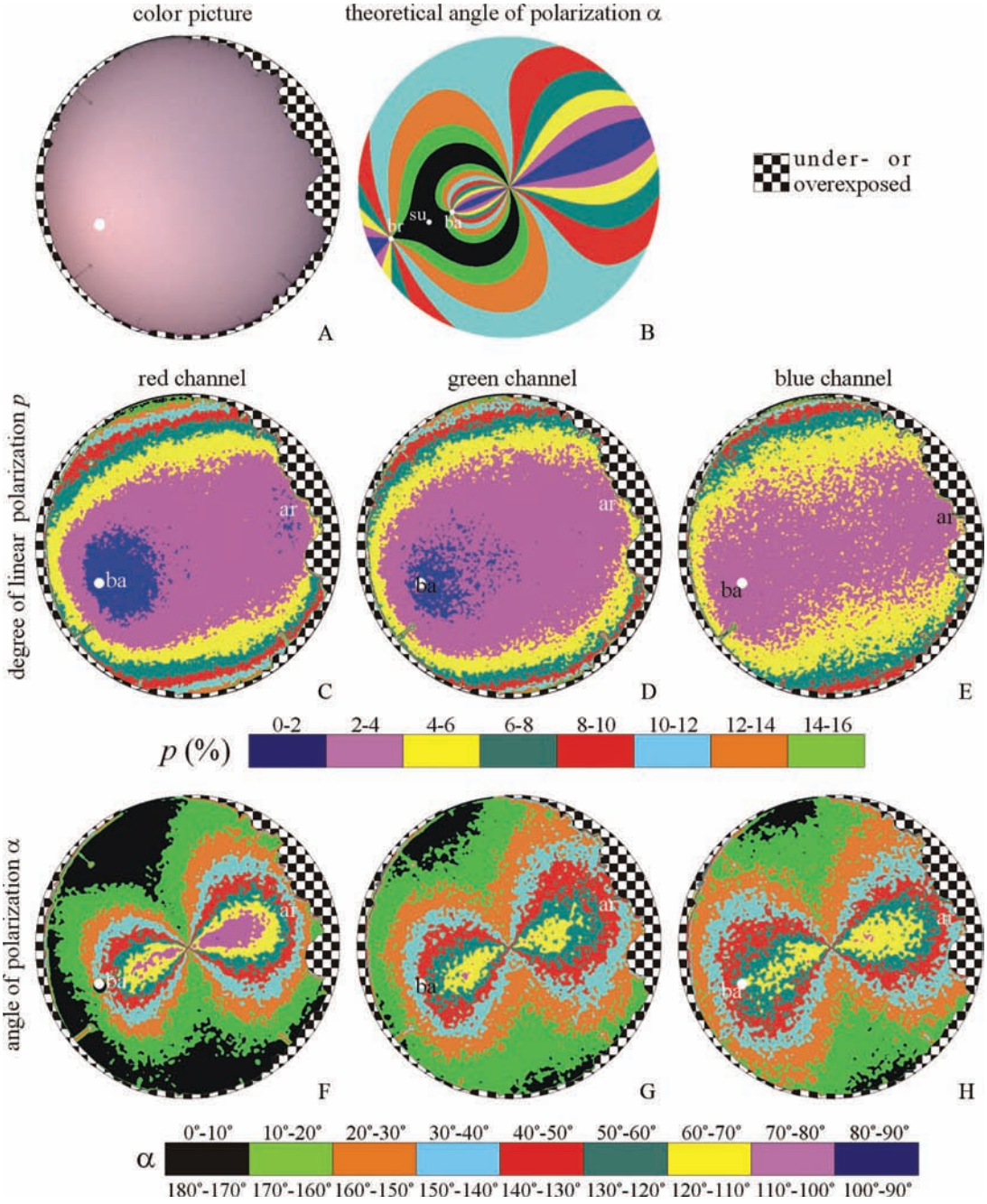

Fig. 3. (Color online) A, Color photograph, C–E, patterns of the degree of linear polarization p, and F–H, angle of polarization α of the reddish smoky sky above Fairbanks (64° 49′ N, 147° 45′ W) measured by full-sky imaging polarimetry in the C, F, red, D, G, green, and E, H, blue parts of the spectrum on 17 August 2005 at 15:01 h (local summer time = UTC − 8). B, Theoretical α pattern of the clear sky calculated on the basis of the model of Berry *et al.*[21] for the same Sun position as in photograph A. The position of the Brewster neutral point is shown by br. In patterns C–H the estimated positions of the Arago and Babinet neutral points are shown by ar and ba, respectively. The optical axis of the fish-eye lens was vertical; thus the horizon and zenith are the perimeter and the center of the circular patterns, respectively. The position of the Sun is represented by a white dot. The underexposed trees near the horizon are marked by a checkered pattern.

The distribution of p in the smoky sky was also atypical (Figs. 3C–3E, 4C–4E): at 90° from the Sun the celestial band with highest p did not occur in the p patterns, and the spatial distribution of p was nearly cylindrically symmetric around the zenith. The p of nonanomalous, clear skies is maximal at 90° from the Sun, and it decreases gradually to zero toward the neutral points (Fig. 5C–5E).

Under normal atmospheric conditions the Arago, Babinet, and Brewster neutral (unpolarized) points of the sky are positioned at the cross sections of the solar and antisolar meridians and the iso-lines with

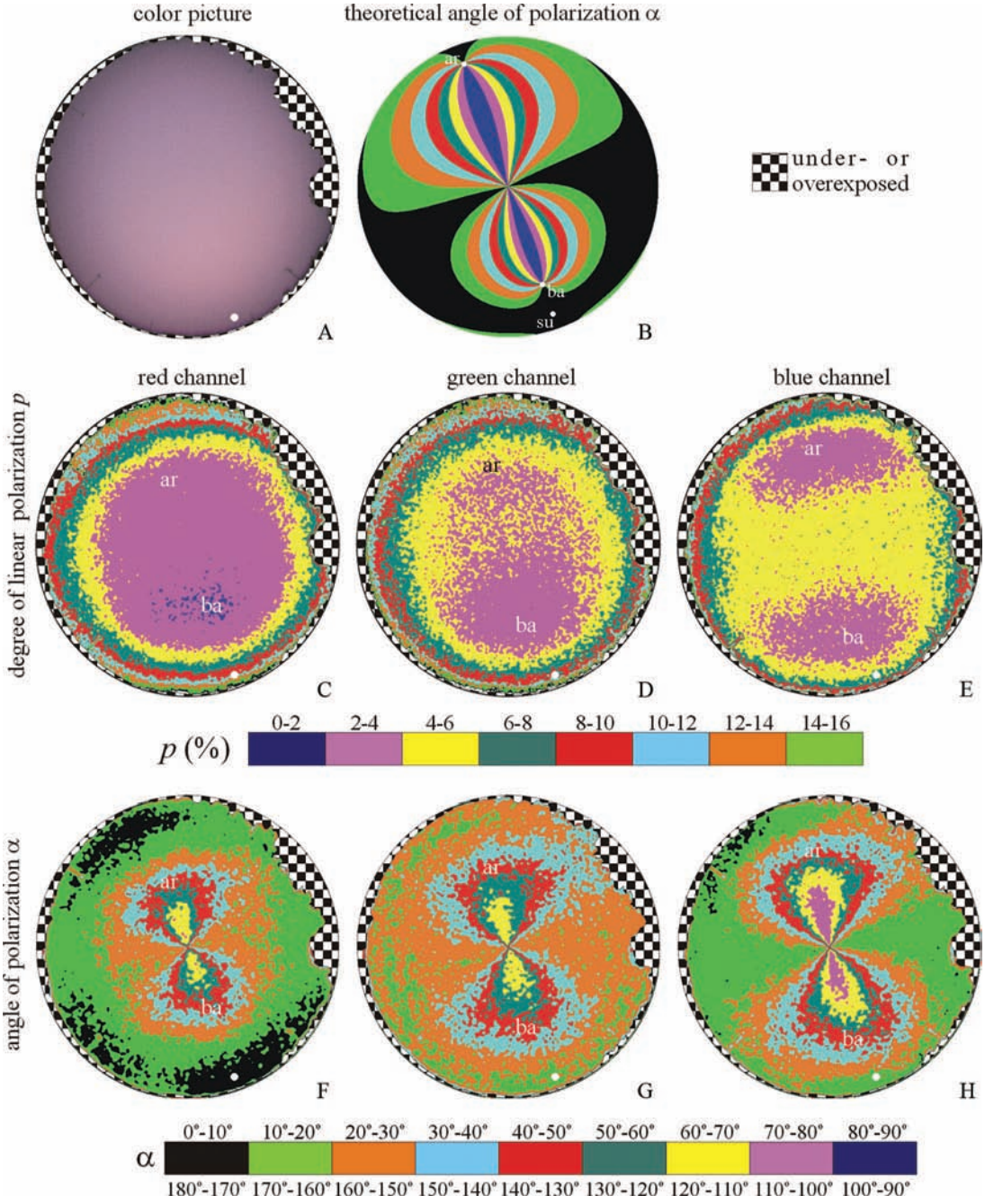

Fig. 4. (Color online) As in Fig. 3 for 20:20 h (= UTC − 8). The position of the invisible Sun occluded by the thick smoke layer near the horizon is represented by a white dot. The solar position was obtained from the online solar position calculator of the U.S. Naval Observatory, Astromonical Applications Department (http://aa.usno.navy.mil) on the basis of the exact time and geographical coordinates of the site of measurements.

$\alpha = \pm 45°$ (Refs. 10, 17, and 22) (Figs. 3F–3H, 4F–4H, 5F–5H). This iso-line between the sky region characterized by $+45° < \alpha < +135°$ and the celestial area characterized by $-45° < \alpha < +45°$ is called the neutral line because it crosses the neutral points. Another anomaly of the smoky sky was that at 15:01 h (Fig. 3F–3H), 16:25 h, and 18:02 h beside the Babinet neutral point the Arago neutral point appeared in the sky, although for the relatively high solar elevations at these times, the Brewster neutral point should have been detectable instead under clear, nonanomalous sky conditions (Fig. 3B). Only at 20:20 h (Figs. 4B, 4F–4H) was this anomaly not observed. Under normal conditions either the Babinet and Brewster points or the Babinet and Arago points (Figs. 5B–5H) are visible.[10,17]

A further deviation from the normal conditions was that in the smoky sky (Figs. 3F–3H, 4F–4H) the zenith angles of the Arago and Babinet neutral points decreased with increasing wavelength, while in the

Table 1. Optical Characteristics of the Anomalous Reddish Smoky Sky above Fairbanks[a]

Sky Condition	Date (2005)	Time (Figure)	Relative Radiance i (%)			Degree of Linear Polarization p (%)			Noisiness n (%) of the Angle of Polarization α		
			Red	Green	Blue	Red	Green	Blue	Red	Green	Blue
Anomalous (Smoky)	17 August	15:01 h (Fig. 3)	74 ± 11	60 ± 8	65 ± 9	4 ± 3	4 ± 3	5 ± 3	20	33	32
Anomalous (Smoky)	17 August	16:25 h	52 ± 11	42 ± 8	47 ± 8	7 ± 5	8 ± 6	6 ± 5	28	48	36
Anomalous (Smoky)	17 August	18:02 h	61 ± 11	48 ± 8	54 ± 8	6 ± 4	7 ± 6	5 ± 3	26	38	39
Anomalous (Smoky)	17 August	20:20 h (Fig. 4)	61 ± 10	49 ± 8	58 ± 9	5 ± 4	6 ± 4	5 ± 3	30	43	29
Normal (Clear)	25 August	21:20 h (Fig. 5)	46 ± 17	52 ± 16	74 ± 13	34 ± 25	25 ± 16	21 ± 15	5	3	6

[a]Rows 1–4: (64° 49′ N, 147° 45′ W) on 17 August 2005 measured at four different times (local summer time = UTC − 8) by full-sky imaging polarimetry in the red, green, and blue parts of the spectrum and averaged over the entire sky. The radiance I is normalized to the highest value I_{max}, resulting in the relative radiance $i = I/I_{max}$. The definition of noisiness n of the angle of polarization α is given in Section 2. Row 5: Optical characteristics of the clear blue sky above the arctic ice cover measured on 25 August 2005 at 21:20 h (= UTC − 8) at the site 78° 28′ N and 149° 9′ W.

normal sky, the zenith angles of the Babinet and Arago points increase with increasing wavelength (Figs. 5B–5H). Furthermore, at 15:01 h (Fig. 3F–3H) in the green part of the spectrum, the Babinet point approximately coincided with the solar position, and in the blue the Babinet point was farther from the zenith than the Sun. These features are anomalous because under normal atmospheric conditions (Fig. 3B) the zenith angle of the Babinet point is always smaller than that of the Sun in all spectral ranges. In Fig. 3G, the Sun is at the border of sky regions with $+45° < \alpha < +135°$ and $-45° < \alpha < +45°$, whereas in Fig. 3H, the Sun is within the eight-shaped sky region characterized by $+45° < \alpha < +135°$, a phenomenon that never occurs under normal conditions.[17]

The noisiness of the patterns of the angle of polarization α (Figs. 3F–3H, 4F–4H) of smoky skies was also considerably different from that of the normal clear sky (Figs. 3B, 4B, 5F–5H). According to Table 1, the noisiness n of the α pattern of smoky skies ranged from 20% to 48%. Contrary to these large n values, under clear-sky conditions the noisiness n of α changed between 3% and 6% (Table 1).

4. Discussion and Conclusions

A. Smoke-Induced Anomalous Sky Polarization above Fairbanks during Forest Fires

The two most useful parameters of skylight polarization in indicating atmospheric conditions are the maximum p_{max} of the degree of linear polarization p and the positions of the neutral points.[10,13] Considering these characteristics, the major attributes of the polarization patterns of cloudless, clear, aerosol-poor, normal skies (Fig. 5) are the following[10,17,22]:

- In daytime the normal skylight is blue, and its color saturation increases with increasing angular distance γ from the Sun and/or anti-Sun. Thus the blueness of the day sky is deepest at 90° from the Sun and/or anti-Sun. Increasing aerosol concentration results in decreasing color saturation.
- The degree of linear polarization p of normal skylight reaches its maximum p_{max} at 90° from the Sun along the antisolar meridian. Aerosols usually decrease p_{max} due to multiple scattering. p_{max} decreases with decreasing wavelength, but its typical values remain high, ranging between 60% and 85%.
- The noisiness n of the angle of polarization α of normal skylight is low.
- The Sun and anti-Sun are always placed in the sky regions characterized by $-45° < \alpha < +45°$.
- The Babinet neutral point is placed along the solar meridian, at approximately 15°–25° above the Sun. The Arago neutral point occurs along the antisolar meridian, at approximately 15°–25° above the anti-Sun.
- The zenith angles of the Arago and Babinet neutral points decrease with decreasing wavelength.
- The symmetry axes of the iso-lines of α (i.e., characterized by α = constant) in the solar and antisolar halves of the sky are parallel to each other and coincide with the solar and antisolar meridians.

The major attributes of the anomalous polarization patterns of the smoky sky in Fairbanks on 17 August 2005 (Figs. 3 and 4) were the following:

- The skylight was reddish.
- The p pattern had approximately a rotational symmetry around the zenith; p of skylight did not reach its maximum at 90° from the Sun (Figs. 3C–3E, 4C–4E).
- p of skylight was drastically reduced due to the smoke particles enhancing multiple scattering: p was not higher than 14%; the maximum of p averaged on the full sky was as low as 8% (Table 1).
- The α noisiness n of skylight polarization was anomalously high (Table 1).
- Depending on wavelength λ and time t, the Sun was anomalously placed in the sky regions with $+45° < \alpha < +135°$ (Fig. 3H).

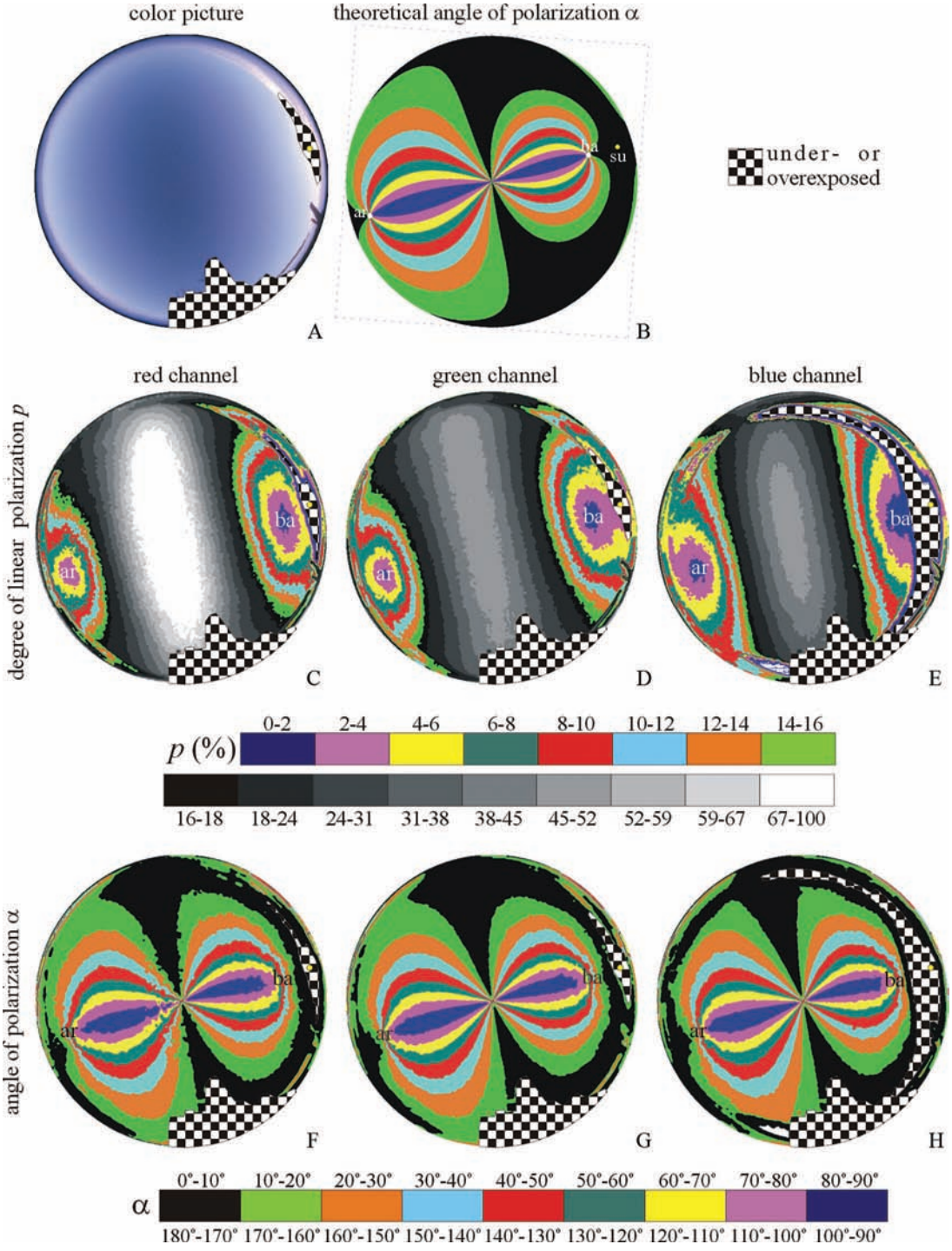

Fig. 5. (Color online) As Fig. 3 for a clear blue sky above the arctic ice cover measured on 25 August 2005 at 21:20 h (= UTC − 8) at the site 78° 28′ N and 149° 9′ W. The position of the Sun visible by the naked eye is represented by a yellow dot. The overexposed sky region around the Sun and the underexposed contour of the icebreaker Oden are marked by a checkered pattern.

- Depending on λ and t, the Babinet neutral point was anomalously positioned below the Sun (Fig. 3H).
- Depending on t, the zenith angles of the Arago and Babinet neutral points changed anomalously with λ (Figs. 3F–3H, 4F–4H).
- In three cases from the four measurements, the Arago point appeared in the sky instead of the Brewster point.

According to Coulson,[10] the extreme sensitivity of the Babinet point to aerosols makes it particularly useful for detecting atmospheric turbidity for whatever cause. In the smoky sky above Fairbanks, we also experienced the anomaly in the position of the Babinet point. From the above, we conclude that the polarization of the sky above Fairbanks on 17 August 2005 was in several aspects anomalous. Note that the

fog itself might have also been induced by the smoke: The smoke particles could function as centers of condensation.

Many polarization-sensitive animals (arthropods, fish, amphibians, reptiles, and birds) use the polarization pattern of skylight for orientation.[17] If this pattern changes drastically, as described in this work, animals orienting on the basis of sky polarization could easily go astray. An anomalous polarization pattern could also reduce the motivation to migrate, such that the invertebrate and vertebrate fauna would avoid migration and potentially be trapped in areas where their survival would be threatened by direct exposure to the fire. We suggest that the disorientation of insects observed by Johnson *et al.*[19] under smoky skies might be the consequence of such anomalous sky polarization. Considering orientation, the most disturbing effect could be that the degree of linear polarization p of light from smoky skies is very low. If p is lower than the species-dependent threshold p^* of polarization sensitivity, the skylight polarization cannot be detected. Honey bees (*Apis mellifera*) and field crickets (*Gryllus campestris*), for example, possess $p^* \approx 10\%$ and 5%, respectively.[17]

Since CO_2 is highly toxic, and thus repellant to insects, one could imagine that the insects observed by Johnson *et al.*[19] became disoriented not only because of the anomalous sky polarization caused by the smoke, but also partly due to the gases released by the forest fire. In the future, it would be worth studying in detail how and why the orientation behavior of animals that use celestial polarization changes at times when the sky is covered by forest fire smoke. It would also be interesting to investigate how their behavior is influenced by dust emissions and volcanic eruptions. Dust alone, for example, fine particles in the air after a storm, would probably have a different effect on insects, because CO_2 and other gases accompanying forest fires would not be present.

B. Earlier Observations on Anomalous Sky Polarization due to Volcanic Dust Clouds

It is well known that the material injected into the upper atmosphere by large volcanic eruptions can cause many optical effects. Occasionally, the sky and/or the disk of the Sun or Moon have been observed to have a green, blue, violet, yellow, or red cast.[10] The dust clouds produced by the four largest volcanic eruptions (Krakatoa, Katmai, Agung, and El Chichon), for example, had the following major effects upon sky polarization:

- The volcanic dust cloud produced by the eruptions of the mountain Krakatoa in the Sunda Straits between Sumatra and Java in 1883 caused a considerable reduction of the degree of linear polarization p of skylight, which could still be observed even about a year after the eruptions.[10] Cornu,[23] for example, measured a maximum p value of only ~5% (instead of the normal 75%) on clear days at 90° from the Sun along the antisolar meridian when the Krakatoa dust cloud was over the observation site. He also observed that p of skylight was lower in the red than in the blue part of the spectrum. The normal situation in the clear atmosphere is the reverse of this. According to Cornu's observations,[23] the Arago, Babinet, and Brewster neutral points were significantly displaced, and he found four other neutral points lying outside the solar–antisolar meridian: One neutral point was found on either side of the Sun at an angle of more than 20° from the Sun at about the same elevation as the Sun. In the green, the neutral points were indistinct, and in the blue, they moved close to the Sun. The other two neutral points were situated symmetrically on either side of the antisolar point and at about the same elevation.
- In 1912, the Alaskan volcano Mount Katmai erupted, and the skylight polarization did not return to its normal state until 1914 (Ref. 10). Kimball,[24] Dorno,[25,26] and Jensen[27,28] observed that p of skylight at 90° from the Sun along the antisolar meridian decreased (by a maximum of 27%) and the positions of the neutral points shifted due to the volcanic dust cloud. The Babinet point, for instance, shifted by up to 17° farther from the Sun.
- In 1963, the Mount Agung volcano erupted on the island of Bali, Indonesia. Shah[29] observed a considerable decrease of p of skylight at the zenith due to the dust cloud in 1963 and 1964 at Ahmedabad, India.
- In 1982, the mountain El Chichon in Mexico broke out. Its effect on sky polarization was thoroughly documented at the Mauna Loa Observatory.[10,12] During the densest period of the dust cloud the Babinet neutral point was positioned at the zenith when the Sun was 3° above the horizon. After sunrise, p of skylight was low ($p_{max} < 20\%$) throughout the day over the entire sky at 700 nm (red). Under normal conditions, the angular distance of the Arago point from the antisolar point was approximately 17°–18° and underwent little change with Sun elevation. Due to the El Chichon dust cloud, this angle of the Arago point from the anti-Sun considerably increased (by over 11° at 700 nm) in comparison with normal conditions. The angle of the Babinet point from the Sun also increased very much (by over 50° at 700 nm). Sometimes the Babinet point completely disappeared, and a second, anomalous neutral point appeared between the Babinet point and the Sun because of the dense turbidity of the atmosphere. The situation had returned more or less to normal by the end of 1983.

C. Earlier Observations on Anomalous Sky Polarization due to Fog, Dust, Smoke, Haze, and Smog

Earlier, researchers observed the following anomalies of sky polarization and neutral points induced by fog, dust, smoke, haze, and smog:

- Under unusual atmospheric conditions, anomalous, additional neutral points have been observed, and in some cases they were located outside the solar–antisolar meridian. In fog or haze over the surfaces of lakes, Soret[30] symmetrically observed one

neutral point on either side of the Sun and the anti-Sun at about the same elevation as the Sun.

- Dust in the atmosphere usually results in a strong decrease of p_{max} of skylight polarization, particularly at the longer wavelengths.[10] The result is that p becomes smaller in the red than in the blue, which is the reverse of the normal situation. In dusty atmospheres, the maximum of p is generally shifted by a few degrees from its normal position (90° from the Sun).
- Under conditions of smoke from agricultural fires prevalent in the low levels of the atmosphere near Davis, California, Coulson[10] observed a significant decrease of p at 400 and 800 nm, especially at the former wavelength, for which p was much smaller than that for the latter. The smoke particles from such low-temperature fires are rich in carbonaceous materials and are thus highly absorbing. The absorption minimizes multiple scattering, which itself would tend to increase p. However, the heavy burden of aerosols in such conditions would be more influential in the polarizational field than would Rayleigh scattering, the result being the low p values observed, particularly at 400 nm.
- Haze and/or photochemical smog considerably decreases p, especially for longer wavelengths due to the effects of aerosols.[10]

Our full-sky imaging polarimetric data gathered in Fairbanks during the Alaskan forest fire season in August 2005 complete these earlier observations and sporadic point-source polarimetric measurements. Since the changes of skylight polarization were induced always by atmospheric aerosols (dust or fog or haze or smog particles) in all mentioned cases, the underlying physics, i.e., scattering of sunlight on aerosol particles, was always the same. Furthermore, the anomalous charateristics of the sky polarization patterns measured by us can explain the disorientation of polarization-sensitive insects observed by Johnson *et al.*[19] during Canadian forest fire seasons. Thus, large-scale forest fires may not only have a direct negative effect on habitat availability and mortality in animal populations but also could influence the animals' ability to navigate and escape from the dangers of the fire itself. On a more regional scale, we cannot exclude that forest fires can have a negative effect on animal migration systems in which migration between different habitats is crucial for the survival of the migrants.[31] Gál *et al.*[32] showed that the polarization pattern of the moonlit clear night sky is practically the same as that of the sunlit clear sky, if the position of the Moon and Sun is the same. Thus we expect that forest fire smoke has similar effects on the sky polarization during day and night.

The financial support received by S. Åkesson and G. Horváth from the Swedish Polar Research Secretariat and from the Swedish Research Council to S. Åkesson is very much acknowledged. G. Horváth is grateful to the German Alexander von Humboldt Foundation for an equipment donation. We thank Rüdiger Wehner (Zoological Institute, University of Zurich, Switzerland) very much for lending us his Nikon-Nikkor fish-eye lens for our imaging polarimetric measurements.

References

1. Y. J. Kaufman, D. Tanré, and O. Boucher, "A satellite view of aerosols in the climate system," Nature **419,** 215–223 (2002).
2. D. F. Yefremov and A. Z. Shvidenko, "Long-term environmental impact of catastrophic forest fires in Russia's Far East and their contribution to global processes," Int. Forest Fire News **32,** 43–49 (2004).
3. F. M. Bréon, "How do aerosols affect cloudiness and climate?" Science **313,** 623–624 (2006).
4. Y. J. Kaufman and I. Koren, "Smoke and pollution aerosol effect on cloud cover," Science **313,** 655–658 (2006).
5. E. S. Kasischke and B. J. Stocks, eds., *Fire, Climate Change and Carbon Cycling in the Boreal Forest,* Ecological Studies Series (Springer-Verlag, 2000).
6. S. E. Page, F. Seigert, J. O. Rieley, H.-D. Boehm, A. Jaya, and S. Limin, "The amount of carbon released from peat and forest fires in Indonesia during 1997," Nature **420,** 61–65 (2002).
7. M. A. Cochrane, "Fire science for rainforests," Nature **421,** 913–919 (2003).
8. P. Aldhous, "Borneo is burning," Nature **432,** 144–146 (2004).
9. E. A. Johnson and K. Miyanishi, *Forest Fires: Behavior and Ecological Effect* (Academic, 2000).
10. K. L. Coulson, *Polarization and Intensity of Light in the Atmosphere* (A. Deepak Publishing, 1988).
11. K. L. Coulson, "Characteristics of skylight at the zenith during twilight as indicators of atmospheric turbidity. 1: Degree of polarization," Appl. Opt. **19,** 3469–3480 (1980).
12. K. L. Coulson, "Effects of the El Chichon volcanic cloud in the stratosphere on the polarization of light from the sky," Appl. Opt. **22,** 2265–2271 (1983).
13. H. Neuberger, "Arago's neutral point: a neglected tool in meteorological research," Bull. Am. Meteorol. Soc. **31,** 119–125 (1950).
14. G. Steinhorst, "Stratospheric aerosol concentration determined by an iterative method from twilight polarization measurements," Beit. Phys. Atmos. **50,** 508–523 (1977).
15. F. E. Volz, "Volcanic turbidity, skylight scattering functions, sky polarization, and twilights in New England during 1983," Appl. Opt. **23,** 2589–2598 (1984).
16. R. Wehner, "Arthropods," in *Animal Homing,* F. Papi, ed. (Chapman & Hall, 1992), p. 45–144.
17. G. Horváth and D. Varjú, *Polarized Light in Animal Vision—Polarization Patterns in Nature* (Springer-Verlag, 2003).
18. R. Muheim, J. B. Phillips, and S. Åkesson, "Polarized light cues underlie compass calibration in migratory songbirds," Science **313,** 837–839 (2006).
19. D. L. Johnson, D. Naylor, and G. Scudder, "Red sky in day, bugs go astray," *Annual Meeting of the Canadian Association of Geographers, Western Division, Lethbridge, Alberta, Canada, 12 March 2005,* Abstracts (2005), p. 45.
20. J. Gál, G. Horváth, V. B. Meyer-Rochow, and R. Wehner, "Polarization patterns of the summer sky and its neutral points measured by full-sky imaging polarimetry in Finnish Lapland north of the Arctic Circle," Proc. R. Soc. London Ser. A **457,** 1385–1399 (2001).
21. M. V. Berry, M. R. Dennis, and R. L. Lee Jr., "Polarization singularities in the clear sky," New J. Phys. **6,** 162 (2004).
22. G. P. Können, *Polarized Light in Nature* (Cambridge U. Press, 1985).
23. A. Cornu, "Observations relatives a la couronne visible actuellement autour du soleil," C. R. Acad. Sci. Paris **99,** 488–493 (1884).

24. H. H. Kimball, "The effect of the atmospheric turbidity of 1912 on solar radiation intensities and skylight polarization," Bull. Meteorological Weather Observatory **5,** 295–312 (1913).
25. C. Dorno, "Himmelshelligkeit, Himmelspolarisation und Sonnenintensität in Davos (1911 bis 1918). I," Meteorologische Zeit. **36,** 109–128 (1919).
26. C. Dorno, "Himmelshelligkeit, Himmelspolarisation und Sonnenintensität in Davos (1911 bis 1918). II," Meteorologische Zeit. **36,** 181–192 (1919).
27. C. Jensen, "Die Himmelsstrahlung," in *Handbuch der Physik* (Springer, 1928), Vol. 19, p. 70–152.
28. C. Jensen, "Die Polarisation des Himmelslichts," in *Handbuch der Geophysik* (Springer, 1942), Vol. 8, p. 527–620.
29. G. M. Shah, "Enhanced twilight glow caused by the volcanic eruption on Bali Island in March and September, 1963," Tellus **21,** 636–640 (1969).
30. J. L. Soret, "Influences des surfaces d'eau sur la polarisation atmospherique et observation de deux points neutres a droite et a gauche de soleil," C. R. Acad. Sci. Paris **107,** 867–870 (1888).
31. T. Alerstam, A. Hedenström, and S. Åkesson, "Long-distance migration: evolution and determinants," Oikos **103,** 247–260 (2003).
32. J. Gál, G. Horváth, A. Barta, and R. Wehner, "Polarization of the moonlit clear night sky measured by full-sky imaging polarimetry at full moon: comparison of the polarization of moonlit and sunlit skies," J. Geophys. Res. D **106,** 22647–22653 (2001).